Hepatic HuR protects against the pathogenesis of non-alcoholic fatty liver disease

Mi Tian
Shandong University School of Medicine: Shandong University Cheeloo College of Medicine
Xinyun Li
Shandong University School of Medicine: Shandong University Cheeloo College of Medicine
Jingyuan Li
Shandong University School of Medicine: Shandong University Cheeloo College of Medicine
Jianmin Yang
Shandong University School of Medicine: Shandong University Cheeloo College of Medicine
Cheng Zhang
Shandong University School of Medicine: Shandong University Cheeloo College of Medicine
Wencheng Zhang (zhangwencheng@sdu.edu.cn)
Shandong University School of Medicine: Shandong University Cheeloo College of Medicine
https://orcid.org/0000-0002-9416-6540

Original investigation

Keywords: HuR, PTEN, NAFLD, liver steatosis, glucose metabolism

Posted Date: November 4th, 2020

DOI: https://doi.org/10.21203/rs.3.rs-97971/v1

Abstract

Background: Liver plays an important role in lipid and glucose metabolism. Human antigen R (HuR) as an RNA regulator protein participates in many disease processes. Here, we investigated the specific role of HuR in hepatic steatosis and glucose metabolism.

Methods: We investigated the level of HuR in liver from mice fed a normal chow diet (NCD) and high fat diet (HFD). Liver specific HuR knockout (HuR^{LKO}) mice were generated and challenged with an HFD. Lipid levels and glucose metabolism index were examined.

Results: HuR was downregulated in livers of HFD-fed mice. HuR^{LKO} mice showed exacerbated HFD-induced hepatic steatosis but improved glucose tolerance as compared with controls. Consistently, HuR inhibited lipid accumulation in hepatocytes. Mechanically, HuR could bind to the mRNA of phosphatase and tensin homology deleted on chromosome 10 (PTEN), thus increasing their stability and translation. Finally, PTEN over-expression alleviated HFD-induced hepatic steatosis in HuR^{LKO} mice.

Conclusion: HuR modulates lipid and glucose metabolism through regulating PTEN expression.

Background

Non-alcoholic fatty liver disease (NAFLD) is becoming the highest morbidity liver disease that leads to end-stage liver lesions with cardiovascular and metabolic comorbidity[1]. It is a pathological process that encompasses a spectrum of liver metabolic disorders starting with non-inflammatory liver steatosis, defined as greater than 5% triglycerides (TG) accumulation in hepatocytes, which then leads to inflammation, fibrosis, and cirrhosis[2].

Steatosis develops due to increased fatty acid (FA) uptake and de novo lipogenesis, which are associated with changes in hepatic glucose metabolism, including enhanced glycolysis and decreased gluconeogenesis[3, 4]. Glucose and lipid metabolism are regulated by multiple mechanisms. The phosphatase and tensin homology deleted on chromosome 10 (PTEN)/phosphoinositide 3 kinase (PI3K)/Akt pathway plays the most important role because of its position downstream of the insulin receptor[5]. PTEN is a bispecific phosphoinositide and protein phosphatase that dephosphorylates phosphatidylinositol-3,4,5-trisphosphate (PtdIns (3,4,5) P3), an effective deactivator of Akt[6]. Liver specific PTEN deficiency promoted NAFLD while improved glucose tolerance[7]. Thus, it is important to understand the regulation of PTEN expression or activity. However, the molecular mechanism involved in PTEN expression has not been fully elucidated.

Human antigen R (HuR), also known as embryonic lethal abnormal vision-like 1 (ELAVL1), is a universally expressed member of the Hu/ELAV family of RNA-binding proteins[8]. As an RNA regulator, HuR selectively binds to the adenylateuridylate-rich elements (AREs) usually found in the 3'-untranslated region (UTR) of its targets via its RNA recognition motifs[9]. Global HuR-deficient mice showed embryonic lethality owing to extraembryonic placenta defects[10]. Our previous study found that mice with adipose-

specific HuR deletion were susceptible to obesity induced by a high fat diet (HFD)[11]. Several studies suggested that HuR regulates cholesterol transportation by protecting against metabolic syndrome-related diseases[12, 13]. However, the specific role of HuR in hepatocytes, particularly in hepatic steatosis and glucose metabolism, has not been explicitly explored.

In this study, we researched the role of HuR in the progression of HFD-induced hepatic steatosis. Liver specific HuR knockout (HuR^{LKO}) mice were generated and challenged with HFD. We found that HuR deletion in liver aggravated HFD-induced hepatic steatosis.

Materials And Methods

Animals

$HuR^{flox/flox}$ (#021431) and albumin-Cre mice (#003574) in a C57BL/6J background were purchased from the Jackson Laboratory (Bar Harbor, ME). HuR^{LKO} mice were generated by crossbreeding $HuR^{flox/flox}$ mice with albumin-Cre mice. The littermate $HuR^{flox/flox}/Cre^{-}$ mice were used as controls (CTR). At age 8 weeks, mice were fed an HFD (D12492; Research Diets) consisting of 60% fat or a normal chow diet (NCD) (D12450B; Research Diets). Body weight was monitored every week. All mice were housed under specific pathogen-free conditions on a 12-h light/12-h dark cycle with food and water freely available. The animal experiment was approved by the Animal Care Committee of Shandong University and was performed in compliance with the Animal Management Rules of the Chinese Ministry of Health (Document No. 55, 2001). All procedures conformed to the guidelines from the NIH Guide for the Care and Use of Laboratory Animals.

Reagents

Bovine serum albumin (BSA, #B2064), oleic acid (OA, #O1008), palmitic acid (PA, #P0500), MG-132(#M7449), chloroquine (CQ, #C6628), actinomycin D (#SBR00013) and TG assay kit (MAK266) were purchased from Sigma. HuR-ARE interaction inhibitor CMLD-2 was purchased from Millipore (#5.38339.0001). The antibodies used were specific for HuR (Millipore, #07-468), Akt (Cell Signaling Technology, #4691), phospho-Akt at Ser473 (Cell Signaling Technology, #4060), PTEN (Cell Signaling Technology, #9188), Tublin (Proteintech, #11224-1-AP), and GAPDH (Cell Signaling Technology, cat #2118). Lentivirus encoding PTEN (Lenti-PTEN) or Lenti-LacZ were from Jikai (Shanghai, China). Adenovirus expressing GFP (AdGFP) and HuR (AdHuR) were from Vigenebio (MD, USA). The insulin ELISA kit was from Mercodia (10-1249-01). The assay kits used to measure serum alanine aminotransferase (ALT), aspartate aminotransferase (AST), nonesterified fatty acids (NEFAs) and total cholesterol (TC) were purchased from Jiancheng Bioengineering Institute (Nanjing, China).

Primary hepatocyte isolation and culture

Mouse primary hepatocytes were isolated from 8-week-old male CTR or HuR^{LKO} mice. In brief, after anesthetization, the liver was perfused through the portal vein with 40 ml warm (37°C) wash buffer (0.4

g/L KCl, 0.06 g/L KH_2PO_4, 8 g/L NaCl, 0.35 g/L $NaHCO_3$, 0.132 g/L $Na_2HPO_4.12H_2O$, 0.1% glucose, 1 mM Hepes, 0.5 mM EDTA) at 5 ml/min with the perfusate exiting through the suprahepatic vena cava, followed with digestion with 20 ml collagenase type II buffer (Gibco, #17101-015). Then hepatocytes were placed in a 10-cm Petri dish. The cell suspension was isolated through a 100-μm filter (Falcon, #352360), and centrifuged at 800 rpm for 5 min. Hepatocytes were purified with 90% Percoll (GE Healthcare Life Sciences, #17-0891-01) and washed twice. Finally, hepatocytes were counted and cultured in high-glucose DMEM (Gibco, USA) containing 10% fetal bovine serum (FBS; BI, USA) at 37 °C in 5% CO_2.

Measurement of glucose tolerance test (GTT) and insulin tolerance test (ITT)

For GTT, mice were fasted for 14-16 h and then received an intraperitoneal (i.p.) injection of glucose (0.75 g/kg body weight). For ITT, mice were fasted for 4-6 h and then received an i.p. injection of insulin (1.5 U/kg body weight). At 0, 15, 30, 60, 90 and 120 min after injection, blood glucose concentrations were measured.

Liver histology

Livers were isolated and fixed in 4% formaldehyde solution and then embedded in paraffin wax. 5-μm sections were cut and stained with hematoxylin and eosin (H&E) and periodic acid-Schiff (PAS). Immunohistochemical staining was performed with HuR antibody (Millipore, #07-468, 1:300). Fixed livers were dehydrated with sucrose and embedded in OCT. Frozen sections of 10 μm were stained with Oil-red O for assessing hepatic steatosis.

RNA-immunoprecipitation (RIP) assay

RIP assay was performed with a Magna RIP kit (Millipore, #17-701). Cell lysates were treated with 5 μg rabbit IgG or HuR antibody, and incubated with magnetic protein A/G beads at 4 °C overnight. The immunoprecipitated protein-RNA complex was washed and incubated with proteinase K buffer (30 min at 55 °C). RNAs were extracted by phenol: chloroform: isoamyl alcohol, and reverse transcription was performed to synthesize cDNA. After PCR by indicated primers listed in **supplementary table1**, the product was subjected to agrose gel electrophoresis.

Quantitative polymerase chain reaction (qPCR)

TRIzol reagent (Invitrogen, Carlsbad, CA) was used to extract total RNAs from liver tissue or cells in according to the manufacturer's protocol. The PrimeScript RT Reagent Kit (Takara Biomedical Technology) was used to reverse-transcribe 1 μg RNA into cDNA. PCR amplification involved the SYBR PCR mix (Bio-Rad). The primer sequences used were listed in **supplementary table1**.

Western blot analysis

Briefly, tissue or cell lysates were run on 10% SDS-PAGE gel, and blots were probed with primary antibodies (1:1000) against HuR, Akt, phosphorylated-Akt (Ser473), PTEN, Tublin and GAPDH. Image J (National Institutes of Health, Bethesda, MD) was used to quantify the intensity of bands.

Statistical analysis

SPSS v23 (SPSS Inc., Chicago, IL) was used for all analyses. All data are expressed as mean ± SEM and passed normality and equal variance tests. The data meet the assumptions of the tests. Comparison of two groups was determined by Student *t* test and multiple groups by one-way ANOVA with Bonferroni post-tests. All statistical tests were two-tailed, and $P < 0.05$ was considered statistically significant.

Results

HuR expression was downregulated in hepatic steatosis

To explore the function of HuR in hepatic steatosis, we evaluated its expression in liver of mice fed with HFD for 24 weeks. qPCR, western blot analysis, and immunohistochemistry showed that HuR level was significantly decreased in livers of mice fed with HFD as compared with controls (**Fig. 1a, b, c**). Therefore, HuR could play a role in the development of NAFLD. Similarly, in HepG2 cells and primary hepatocytes stressed with palmitic acid and oleic acid (PO), HuR protein level was also downregulated (**Fig. 1d, e**). However, the mRNA level of HuR was not significantly regulated in primary hepatocytes stimulated with PO (**Fig. 1f**), which suggests that the downregulation of HuR protein might be a post-translational regulation mechanism. To verify this hypothesis, primary hepatocytes were treated with PO and the proteasome inhibitor MG132 or the lysosome inhibitor chloroquine (CQ). Downregulation of HuR under PO stimulation was prevented by CQ treatment (**Fig. 1g**), suggesting that PO induced HuR reduction via lysosomal degradation in hepatocytes.

Liver specific HuR deletion aggravated HFD-induced hepatic steatosis

To assess the role of HuR specifically in liver, liver specific HuR-knockout (HuR^{LKO}) mice were generated (**Fig. 2a**). The lack of HuR in mouse liver tissue was confirmed by qPCR (**Fig. 2b**). HuR protein expression was significantly decreased in liver but not in other tissues from HuR^{LKO} mice (**Fig. 2c**), which was further confirmed by immunohistochemistry assay (**Fig. 2d**).

The 8-week old control and HuR^{LKO} mice were fed a normal chow diet (NCD) or HFD for 24 weeks. HuR^{LKO} mice did not show overt abnormalities with the NCD (**Fig.3a-f**). However, under the HFD, HuR^{LKO} mice gained less body weight, but greater liver weight/body weight (LW/BW) ratio compared with controls (**Fig. 3a, b**). Importantly, HuR^{LKO} mice showed exacerbated HFD-induced hepatic steatosis, as indicated by lipid content (TG, NEFAs, and TC) (**Fig. 3c, d, e**). The greater lipid accumulation in HuR^{LKO} with the HFD was evident by H&E and Oil-red O staining (**Fig. 3f**).

In addition, the mRNA levels of lipid metabolism-associated markers were measured. HuR deletion increased the mRNA levels of fatty acid uptake markers such as CD36 and Fabp1, and lipogenesis markers including Fas, Acca, PPARr and Srebf1 (**Fig. 3g**). The levels of the key enzymes controlling liver fatty acid β-oxidation (PPARα and UCP2) were reduced (**Fig. 3g**). Meanwhile, HuR deficiency increased the expression of the cholesterol metabolism molecule, Hmgcr and the inflammatory cytokines such as interleukin 1 beta (IL-1β), interleukin 6 (IL-6) and tumor necrosis factor α (TNFα) (**Fig. 3g**). Besides, the serum ALT and AST levels were increased in HuR^{LKO} mice compared with controls under HFD (**Fig. 3h**). These data suggested that HFD-induced lipid accumulation and inflammation were exaggerated after HuR deletion in the liver.

Hepatic specific HuR deletion alleviated HFD-impaired glucose tolerance

Hepatosteatosis is usually closely related to impaired glucose tolerance. However, fasting glucose and insulin levels were significantly decreased in HuR^{LKO} mice compared with controls under HFD (**Fig. 4a, b**). Glucose tolerance tests (GTT) and insulin tolerance tests (ITT) also indicated that HuR^{LKO} mice exhibited improved glucose and insulin tolerance under HFD (**Fig. 4c, d**), which was confirmed by insulin-stimulated Akt Ser473 analysis in liver, skeletal muscle, and adipose tissue (**Fig. 4e, f**). Furthermore, HuR deletion increased the mRNA levels of glycolysis markers including Gck, Pkm2 and Hk2, but decreased the expression of gluconeogenesis markers such as Pepck, Fbp1, and G6pase (**Fig. 4h**). However, the liver glycogen content was not affected by HuR knockout (**Fig. 4g**). Taken together, hepatic specific HuR deletion alleviated HFD-impaired glucose tolerance.

HuR inhibited lipid accumulation in hepatocytes

To determine the role of HuR in lipid accumulation *in vitro*, hepG2 cells were infected with adenovirus expressing HuR followed by PO treatment. PO-induced lipid accumulation was attenuated by HuR over-expression (**Fig. 5a, b**). Consistently, primary hepatocytes from HuR-knockout mice aggravated PO-induced lipid accumulation compared with controls (**Fig. 5c, d**). In primary hepatocytes stimulated with PO, HuR knockout significantly increased lipogenesis, fatty acid uptake, and inflammation and decreased fatty acid β-oxidation (**Fig. 5e**), which was consistent with the data from HuR^{LKO} mice under the HFD. Thus, HuR regulates lipid metabolism in hepatocytes *in vitro*.

HuR regulates PTEN mRNA stability

HuR knockout in liver impaired lipid metabolism and aggravated the fatty liver but improved insulin resistance in mice, the phenotype of which was similar with that from hepatic specific PTEN knockout mice[7,14]. Thus, we examined whether PTEN is a target gene of HuR. The expression of PTEN was decreased in HFD mice and PO-stimulated primary hepatocytes (**Fig. 6a, b**), which was consistent with HuR expression pattern. HuR deficiency reduced the level of PTEN mature mRNA but not affect its pre-mRNA level (**Fig. 6c, d, e**). Besides, PTEN protein level was decreased by HuR knockout and increased by HuR over-expression (**Fig. 6f**). We examined the PTEN mRNA sequence and identified 34 conserved adenylateuridylate-rich elements (AREs) in the 3'-UTR of mouse PTEN mRNA. The interaction between

HuR and its target mRNAs could be disrupted by CMLD-2, which reduced the PTEN protein level (**Fig. 6g**). RNA immunoprecipitation assay demonstrated that HuR could bind to PTEN mRNA (**Fig. 6h**). Also, half-life assay further confirmed that HuR over-expression increased PTEN mRNA stability (**Fig. 6i**). Taken together, HuR could bind to PTEN mRNA and regulate its stability.

HuR regulates hepatocyte steatosis through PTEN

To examine whether HuR regulates hepatocyte steatosis through PTEN, control and HuR^{LKO} mice were injected with the lentivirus encoding LacZ (Lenti-LacZ) or PTEN (Lenti-PTEN) at week 8 of HFD. PTEN protein level was significantly increased in Lenti-PTEN groups (**Fig. 7a**). As expected, body weight and fasting blood glucose and insulin levels were significantly increased in HuR^{LKO} mice treated with Lenti-PTEN compared with Lenti-LacZ (**Fig. 7b, c, d**). Moreover, PTEN over-expression significantly decreased the LW/BW ratio, TG, NEFA and TC levels in HuR^{LKO} mice (**Fig. 7e, f, g, h**). H&E and Oil-red O staining revealed greatly decreased lipid deposition in liver of HuR^{LKO} mice treated with Lenti-PTEN (**Fig. 7i**). Also, Lenti-PTEN decreased the mRNA levels of genes associated with lipogenesis, FA uptake, cholesterol synthesis and glycolysis, and increased the expression of genes related to FA β-oxidation and gluconeogenesis in HuR^{LKO} mice (**Fig. 7j**). In addition, PTEN over-expression significantly attenuated PO-induced lipid deposition in hepatocytes (**Fig. 7l**), which further support the *in vivo* conclusion. In summary, hepatic HuR may modulate lipid and glucose metabolism by regulating the expression of PTEN.

Discussion

In this study, we examined the effect of liver specific HuR deletion on NAFLD. HuR^{LKO} mice were susceptible to the development of HFD-induced hepatic steatosis, but also displayed improved systemic insulin sensitivity. Mechanically, HuR could bind to the 3'UTR of PTEN mRNA and increased its stability and translation. PTEN over-expression alleviated HFD-induced hepatic steatosis in HuR^{LKO} mice. Thus, HuR may play an important role in glycolipid metabolism by regulating the expression of PTEN.

HuR, a member of RNA-binding proteins, mediates the expression of various proteins by modulating their mRNA stability and translational efficiency[15]. Through its post-transcriptional effect on specific targets, HuR is involved in the cellular response to proliferative, stress, apoptotic, differentiation, senescence, inflammatory and immune stimuli[16]. Recent studies reported that HuR stabilized cannabinoid receptor 1 and promoted cannabinoid receptor-mediated infiltration of bone-marrow monocytes and macrophages in chronic liver injury[17]. In human hepatocellular carcinoma, elevated cytoplasmic HuR level induced by TIP30 bound to p53 mRNA 3’UTR and induced apoptosis via stabilization of p53 mRNA[18]. In this study, we generated liver specific HuR knockout mice and found that HuR could protect against HFD-induced hepatic steatosis through PTEN, which broadens the biological functions of HuR.

The PTEN/Akt pathway plays a determinant role in the regulation of lipid and glucose metabolism. It is important to explore the regulation of PTEN activity and expression. The catalytic activity of PTEN can be modulated post-translationally by acetylation and oxidation. Histone acetyltransferase and p300/CBP-

associated factor-mediated acetylation results in the inactivation of PTEN activity[19], which could also be caused by reactive oxygen species via oxidative stress-induced formation of a disulphide bond between Cys71 and Cys124[20, 21]. In addition, different phosphorylation sites are regulated to control the activity of PTEN[22–24]. PTEN expression can be upregulated by many transcription factors such as PPARγ[25] and early growth-response protein 1 (EGR1) [26]. Besides, numerous miRNAs including miR-19 and miR-21 could reduce PTEN levels in different diseases[27, 28]. Here we demonstrated that HuR, an mRNA-binding protein, could bind to the 3'UTR of PTEN mRNA and increased its stability and translation, which enhances our understanding of the regulatory mechanisms of PTEN expression.

Steatosis develops from increased de novo lipogenesis, FA uptake and decreased very low-density lipoprotein export[7]. This process is closely linked with changes in hepatic glucose metabolism, including enhanced glycolysis (whose products are essentially used for de novo lipogenesis), as well as decreased gluconeogenesis. Alterations of a single organ can lead to marked phenotypical changes in the metabolic status of organisms via a crosstalk between the liver and peripheral organs. Here we found that hepatic specific HuR deletion aggravated HFD-induced hepatic steatosis in mice but also improved systemic glucose tolerance and insulin sensitivity. The phenotype was similar with liver specific PTEN knockout mice[7, 14]. We demonstrated that PTEN is the target gene of HuR, which further confirmed the PTEN/Akt mechanism in glycolipid metabolism.

Conclusion

In summary, the present study first demonstrated that HuR functions as an important regulator of lipid and glucose metabolism by targeting PTEN to increase its mRNA stability. Liver specific HuR deletion aggravated HFD-induced hepatic steatosis, which indicates that HuR may be a potential therapeutic target for NAFLD.

Abbreviations

ALT, alanine aminotransferase; AST, aspartate aminotransferase; BSA, bovine serum albumin; BW, body weight, GTT, glucose tolerance test; G6Pase, Glucose 6-phosphatase; HFD, high-fat diet; LW, liver weight; LW/BW, liver/body weight ratio; NAFLD, nonalcoholic fatty liver disease; NCD, normal chow diet; NEFA, nonesterified fatty acid; OA, oleic acid; PA, palmitic acid; PEPCK, phosphoenolpyruvate carboxy kinase; PTEN, phosphatase and tensin homology deleted on chromosome 10; PO, palmitic acid and oleic acid; PPAR, peroxisome proliferator-activated receptor; TC, total cholesterol; TG, triglycerides

Declarations

Acknowledgements

Not applicable.

Authors contributions

M.T. and J.L. designed and performed the research. X.L. and J.Y. analyzed data, C.Z. and W.Z. conceived the project, reviewed the data, and wrote the manuscript. All authors discussed and commented on the paper.

Funding

This work was supported by the National Natural Science Foundation of China (no. 81970198, 81770473) and the Taishan Scholar Project of Shandong Province of China (no. tsqn20161066).

Availability of data and materials

All data generated or analyzed during this study are included in this published article.

Ethics approval and consent to participate

The animal experiment was approved by the Animal Care Committee of Shandong University and was performed in compliance with the Animal Management Rules of the Chinese Ministry of Health (Document No. 55, 2001). All procedures conformed to the guidelines from the NIH Guide for the Care and Use of Laboratory Animals. **Consent for publication**

Not applicable.

Competing interests

The authors declare that they have no competing interests.

Author details

[1]The Key Laboratory of Cardiovascular Remodeling and Function Research, Chinese Ministry of Education, Chinese National Health Commission and Chinese Academy of Medical Sciences, The State and Shandong Province Joint Key Laboratory of Translational Cardiovascular Medicine, Department of Cardiology, Qilu Hospital, Cheeloo College of Medicine, Shandong University, Jinan, China

References

1. Cai J, Zhang XJ, Li H. Progress and challenges in the prevention and control of nonalcoholic fatty liver disease. Med Res Rev 2019;39:328-348.
2. Arab JP, Arrese M, Trauner M. Recent Insights into the Pathogenesis of Nonalcoholic Fatty Liver Disease. Annu Rev Pathol 2018;13:321-350.
3. Horie Y, Suzuki A, Kataoka E, Sasaki T, Hamada K, Sasaki J et al. Hepatocyte-specific Pten deficiency results in steatohepatitis and hepatocellular carcinomas. J Clin Invest 2004;113:1774-83.
4. Qiu W, Federico L, Naples M, Avramoglu RK, Meshkani R, Zhang J, et al. Phosphatase and tensin homolog (PTEN) regulates hepatic lipogenesis, microsomal triglyceride transfer protein, and the

secretion of apolipoprotein B-containing lipoproteins. Hepatology 2008;48:1799-809.

5. Song MS, Salmena L, Pandolfi PP. The functions and regulation of the PTEN tumour suppressor. Nat Rev Mol Cell Biol 2012;13:283-96.
6. Maehama T, Dixon JE. The tumor suppressor, PTEN/MMAC1, dephosphorylates the lipid second messenger, phosphatidylinositol 3,4,5-trisphosphate. J Biol Chem 1998;273:13375-8.
7. Peyrou M, Bourgoin L, Poher AL, Altirriba J, Maeder C, Caillon A, et al. Hepatic PTEN deficiency improves muscle insulin sensitivity and decreases adiposity in mice. J Hepatol 2015;62:421-9.
8. Ma WJ, Cheng S, Campbell C, Wright A and Furneaux H. Cloning and characterization of HuR, a ubiquitously expressed Elav-like protein. J Biol Chem 1996;271:8144-51.
9. Chen CY, Xu N, Shyu AB. Highly selective actions of HuR in antagonizing AU-rich element-mediated mRNA destabilization. Mol Cell Biol 2002;22:7268-78.
10. Katsanou V, Milatos S, Yiakouvaki A, Sgantzis N, Kotsoni A, Alexiou M, et al. The RNA-binding protein Elavl1/HuR is essential for placental branching morphogenesis and embryonic development. Mol Cell Biol 2009;29:2762-76.
11. Li J, Gong L, Liu S, Zhang Y, Zhang C, Tian M, et al. Adipose HuR protects against diet-induced obesity and insulin resistance. Nat Commun 2019;10:2375.
12. Singh AB, Dong B, Kraemer FB, Xu Y, Zhang Y, Liu J. Farnesoid X Receptor Activation by Obeticholic Acid Elevates Liver Low-Density Lipoprotein Receptor Expression by mRNA Stabilization and Reduces Plasma Low-Density Lipoprotein Cholesterol in Mice. Arterioscler Thromb Vasc Biol 2018;38:2448-2459.
13. Ramírez CM, Lin CS, Abdelmohsen K, et al. RNA binding protein HuR regulates the expression of ABCA1. J Lipid Res 2014;55:1066-76.
14. Stiles B, Wang Y, Stahl A, Goedeke L, Yoon JH, Madrigal-Matute J, et al. Liver-specific deletion of negative regulator Pten results in fatty liver and insulin hypersensitivity [corrected]. Proc Natl Acad Sci U S A 2004;101:2082-7.
15. Burkhart RA, Pineda DM, Chand SN, Romeo C, Londin ER, Karoly ED, et al. HuR is a post-transcriptional regulator of core metabolic enzymes in pancreatic cancer. RNA Biol 2013;10:1312-23.
16. Srikantan S, Gorospe M. HuR function in disease. Front Biosci (Landmark Ed) 2012;17:189-205.
17. Chang N, Duan X, Zhao Z, Tian L, Ji X, Yang L, et al. Both HuR and miR-29s regulate expression of CB1 involved in infiltration of bone marrow monocyte/macrophage in chronic liver injury. J Cell Physiol 2020;235:2532-2544.
18. Zhao J, Chen J, Lu B, Dong L, Wang H, Bi C,et al. TIP30 induces apoptosis under oxidative stress through stabilization of p53 messenger RNA in human hepatocellular carcinoma. Cancer Res 2008;68:4133-41.
19. Yim EK, Peng G, Dai H, Hu R, Li K, Lu Y, et al. Rak functions as a tumor suppressor by regulating PTEN protein stability and function. Cancer Cell 2009;15:304-14.

20. Lee SR, Yang KS, Kwon J, Lee C, Jeong W, Rhee SG. Reversible inactivation of the tumor suppressor PTEN by H2O2. J Biol Chem 2002;277:20336-42.
21. Silva A, Yunes JA, Cardoso BA, Martins LR, Jotta PY, Abecasis M, et al. PTEN posttranslational inactivation and hyperactivation of the PI3K/Akt pathway sustain primary T cell leukemia viability. J Clin Invest 2008;118:3762-74.
22. Rabinovsky R, Pochanard P, McNear C, Brachmann SM, Duke-Cohan JS, Garraway LA, et al. p85 Associates with unphosphorylated PTEN and the PTEN-associated complex. Mol Cell Biol 2009;29:5377-88.
23. Vazquez F, Grossman SR, Takahashi Y, Rokas MV, Nakamura N, Sellers WR. Phosphorylation of the PTEN tail acts as an inhibitory switch by preventing its recruitment into a protein complex. J Biol Chem 2001;276:48627-30.
24. Liang K, Esteva FJ, Albarracin C, Stemke-Hale K, Lu Y, Bianchini G, et al. Recombinant human erythropoietin antagonizes trastuzumab treatment of breast cancer cells via Jak2-mediated Src activation and PTEN inactivation. Cancer Cell 2010;18:423-35.
25. Patel L, Pass I, Coxon P, Downes CP, Smith SA, Macphee CH. Tumor suppressor and anti-inflammatory actions of PPARgamma agonists are mediated via upregulation of PTEN. Curr Biol 2001;11:764-8.
26. Virolle T, Adamson ED, Baron V, Birle D, Mercola D, Mustelin T, et al. The Egr-1 transcription factor directly activates PTEN during irradiation-induced signalling. Nat Cell Biol 2001;3:1124-8.
27. Xiao C, Srinivasan L, Calado DP, Patterson HC, Zhang B, Wang J, et al. Lymphoproliferative disease and autoimmunity in mice with increased miR-17-92 expression in lymphocytes. Nat Immunol 2008;9:405-14.
28. Meng F, Henson R, Wehbe-Janek H, Ghoshal K, Jacob ST, Patel T. MicroRNA-21 regulates expression of the PTEN tumor suppressor gene in human hepatocellular cancer. Gastroenterology 2007;133:647-58.

Figures

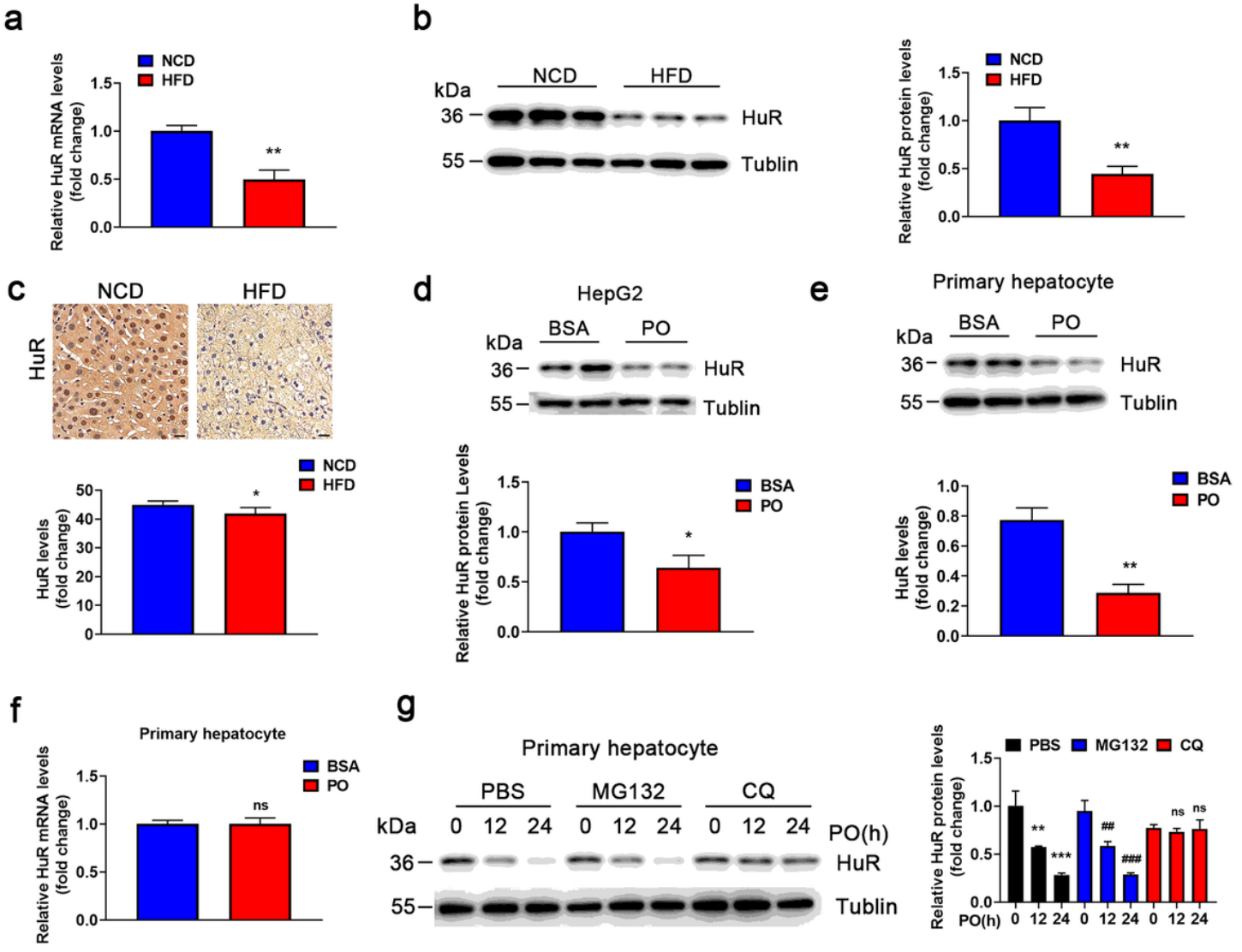

Figure 1

HuR expression was downregulated in hepatic steatosis. (a) qPCR analysis of HuR mRNA expression in liver from C57BL/6J mice fed a normal chow diet (NCD) or high-fat diet (HFD) for 24 weeks (n=5). **P<0.01 vs NCD. (b) Western blot analysis of HuR protein level in liver from C57BL/6J mice fed an NCD or HFD for 24 w (n=5). **P<0.01 vs NCD. (c) Immunohistochemical staining of HuR protein in liver from NCD- and HFD-fed mice (n=5). *P<0.05 vs NCD. Scale bar, 20 μm. Western blot analysis of HuR protein level in HepG2 cells (d) and mouse primary hepatocytes (e) stimulated with bovine serum albumin (BSA) or PO (0.5 mM palmitic acid and 1.0 mM oleic acid) for 24 h (n=5). *P<0.05, **P<0.01 vs BSA. (f) qPCR analysis of HuR mRNA level in primary hepatocytes stimulated with BSA or PO for 24 h. (g) Primary hepatocytes were treated with PO and phosphate-buffered saline (PBS), MG132 or chloroquine (CQ) for 0, 12, or 24 h. Western blot analysis of HuR was shown (n=3). **P<0.01, ***P<0.001, vs PO and PBS at 0 h. ##P<0.01, ###P<0.001 vs PO and MG132 at 0 h.

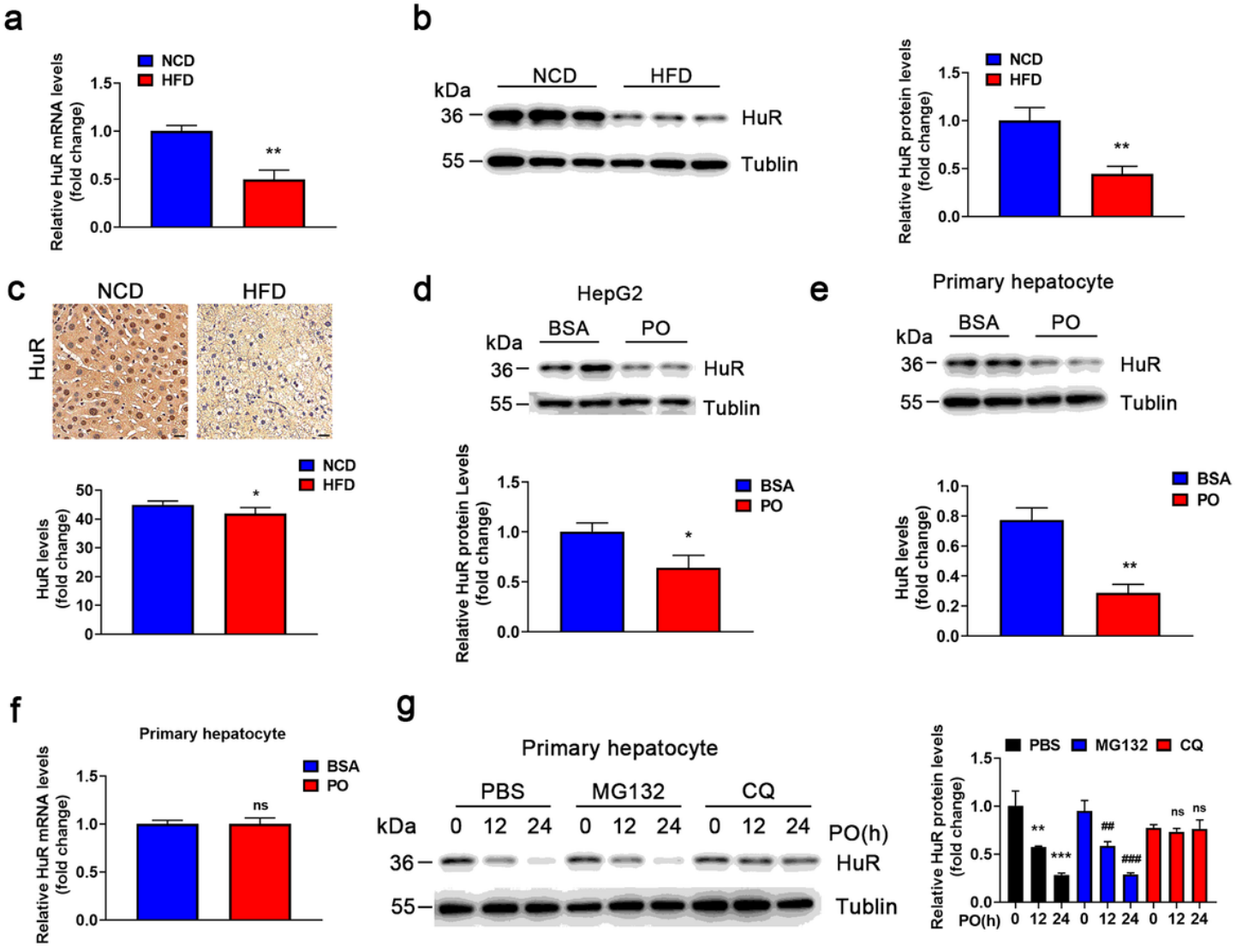

Figure 1

HuR expression was downregulated in hepatic steatosis. (a) qPCR analysis of HuR mRNA expression in liver from C57BL/6J mice fed a normal chow diet (NCD) or high-fat diet (HFD) for 24 weeks (n=5). **P<0.01 vs NCD. (b) Western blot analysis of HuR protein level in liver from C57BL/6J mice fed an NCD or HFD for 24 w (n=5). **P<0.01 vs NCD. (c) Immunohistochemical staining of HuR protein in liver from NCD- and HFD-fed mice (n=5). *P<0.05 vs NCD. Scale bar, 20 μm. Western blot analysis of HuR protein level in HepG2 cells (d) and mouse primary hepatocytes (e) stimulated with bovine serum albumin (BSA) or PO (0.5 mM palmitic acid and 1.0 mM oleic acid) for 24 h (n=5). *P<0.05, **P<0.01 vs BSA. (f) qPCR analysis of HuR mRNA level in primary hepatocytes stimulated with BSA or PO for 24 h. (g) Primary hepatocytes were treated with PO and phosphate-buffered saline (PBS), MG132 or chloroquine (CQ) for 0, 12, or 24 h. Western blot analysis of HuR was shown (n=3). **P<0.01, ***P<0.001, vs PO and PBS at 0 h. ##P<0.01, ###P<0.001 vs PO and MG132 at 0 h.

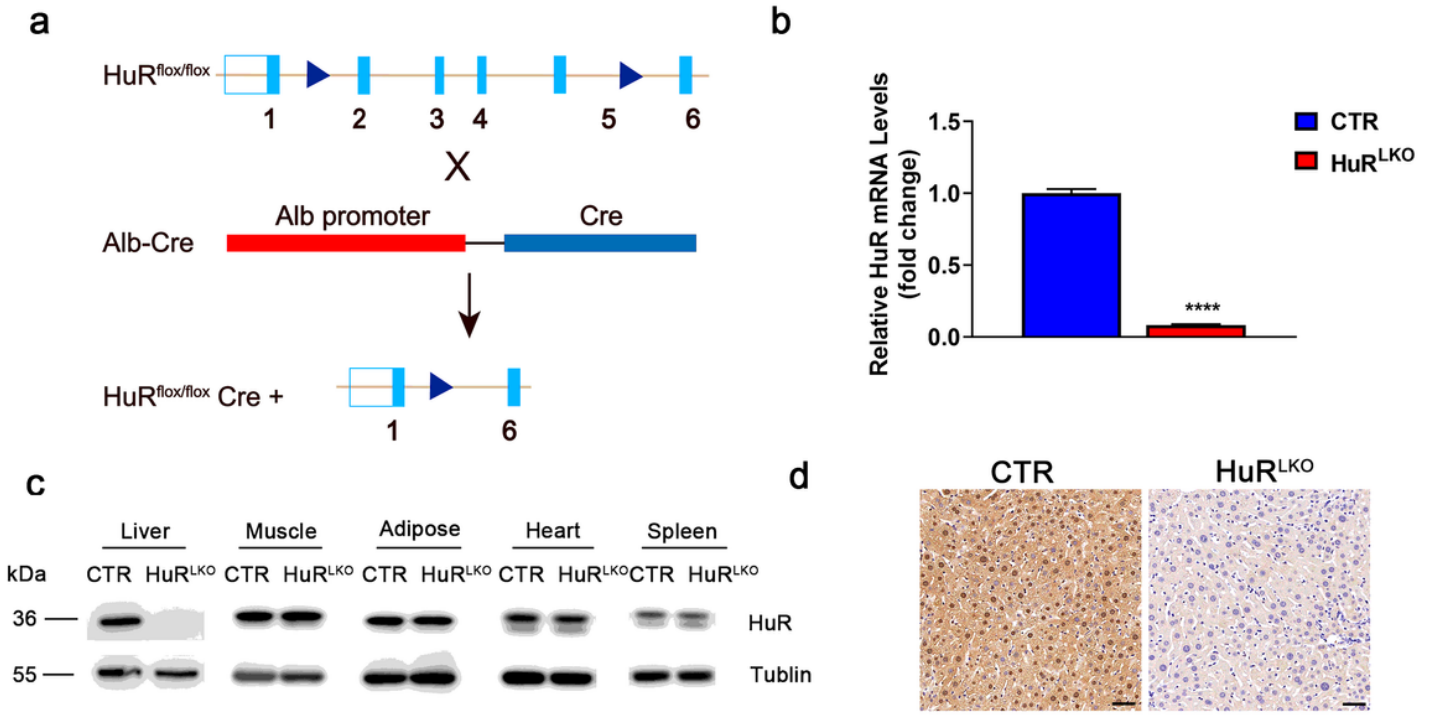

Figure 2

Generation of liver-specific HuR-knockout mice. (a) Schematic diagram of transgenic mice used to generate HuRLKO mice. (b) Quantitative PCR analysis of HuR mRNA level in liver of control and HuRLKO mice (n=5). ****P<0.0001 vs CTR. (c) Western blot analysis of HuR protein level in tissues from CTR and HuRLKO mice. (d) Immunohistochemical staining of HuR protein in liver from CTR and HuRLKO mice. Scale bar, 50 μm.

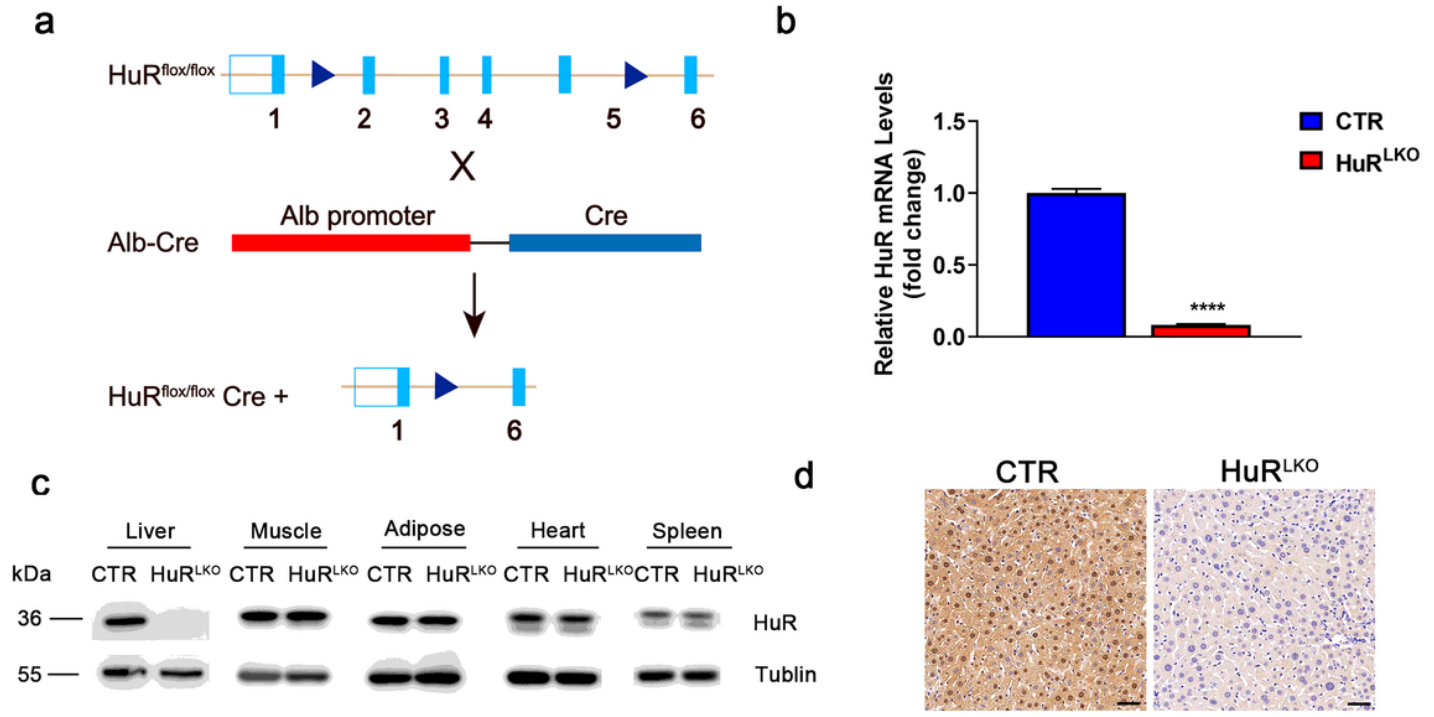

Figure 2

Generation of liver-specific HuR-knockout mice. (a) Schematic diagram of transgenic mice used to generate HuRLKO mice. (b) Quantitative PCR analysis of HuR mRNA level in liver of control and HuRLKO mice (n=5). ****P<0.0001 vs CTR. (c) Western blot analysis of HuR protein level in tissues from CTR and HuRLKO mice. (d) Immunohistochemical staining of HuR protein in liver from CTR and HuRLKO mice. Scale bar, 50 μm.

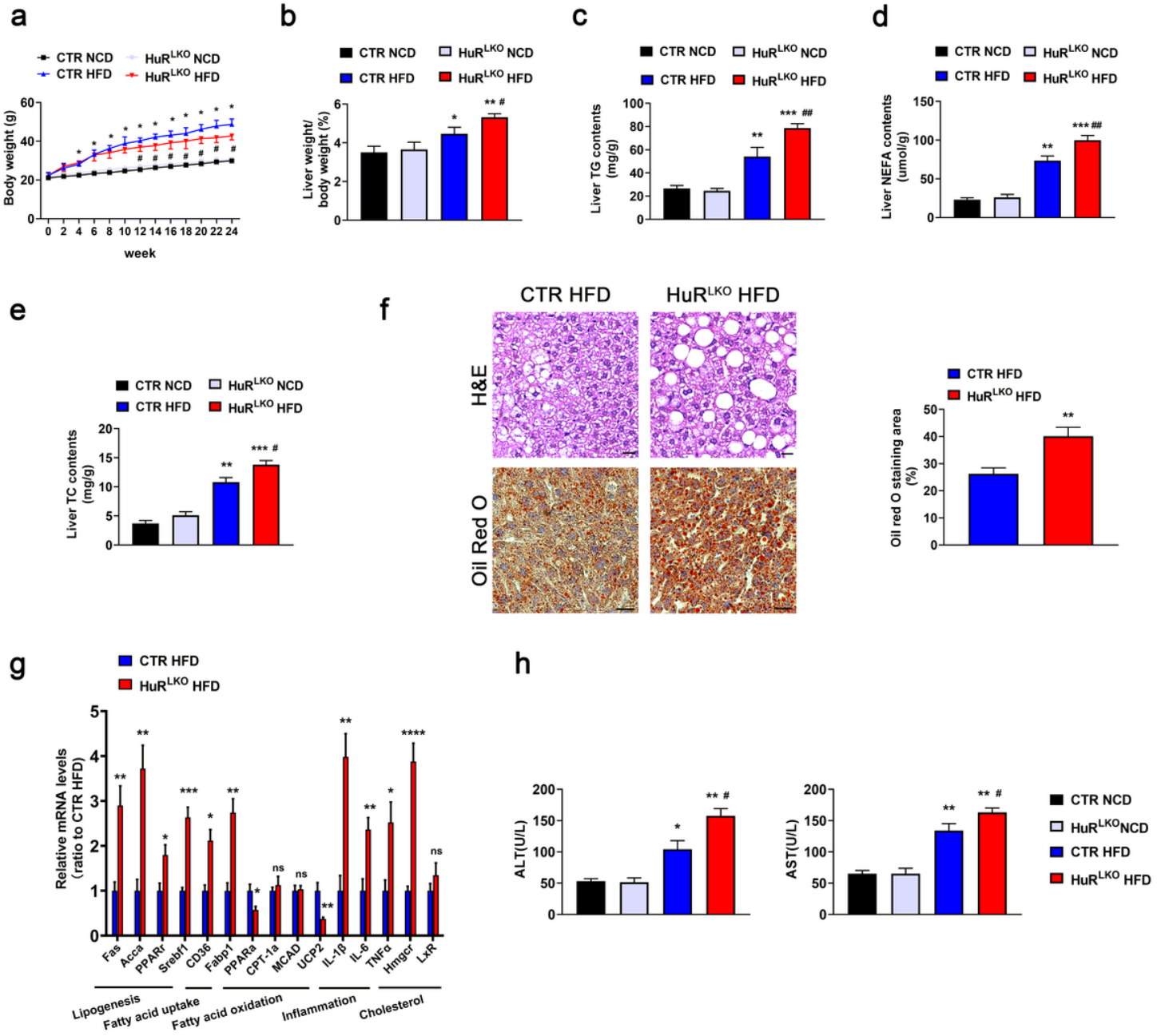

Figure 3

Liver specific HuR deletion aggravated HFD-induced hepatic steatosis. Control and HuRLKO mice were fed a normal chow diet (NCD) or HFD for 24 w. (a) Body weight of mice in different groups (n=10). *P<0.05 vs CTR NCD, #P<0.05 vs CTR HFD. (b) Liver weight to body weight ratio of mice in different groups (n=10). *P<0.05, **P<0.01 vs CTR NCD, #P<0.05 vs CTR HFD. Triglycerides (TG) (c), non-esterified fatty acid (NEFA) (d) and cholesterol (TC) (e) in liver of mice (n=10). **P<0.01, ***P<0.001 vs CTR NC, #P<0.05, ##P<0.01 vs CTR HFD. (f) Hematoxylin and eosin (H&E, top)-stained and Oil Red O (bottom)-stained liver sections from mice. Scale bar, 20 μm. Quantitative analysis (right) of the mean Oil-red O-staining area (n =10). **P<0.01 vs CTR HFD. (g) Relative mRNA levels of indicated molecules in the liver

of mice (n=5). *P<0.05, **P<0.01, ***P<0.001, ****P<0.0001 vs CTR HFD. (h) Serum levels of alanine transaminase (ALT) and aspartate aminotransferase (AST) (n=10). *P<0.05, **P<0.01 vs CTR NCD, #P<0.05 vs CTR HFD.

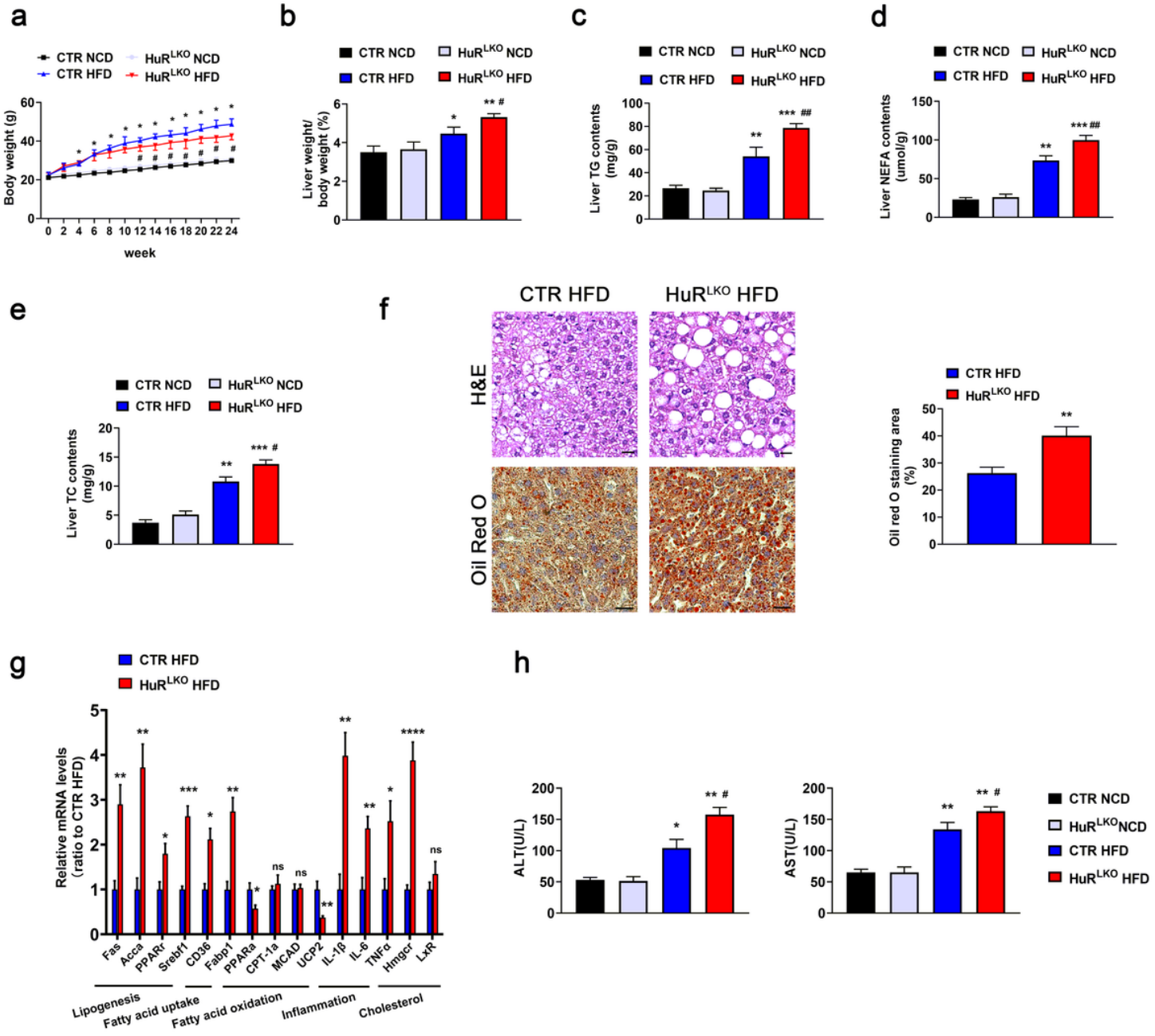

Figure 3

Liver specific HuR deletion aggravated HFD-induced hepatic steatosis. Control and HuRLKO mice were fed a normal chow diet (NCD) or HFD for 24 w. (a) Body weight of mice in different groups (n=10). *P<0.05 vs CTR NCD, #P<0.05 vs CTR HFD. (b) Liver weight to body weight ratio of mice in different groups (n=10). *P<0.05, **P<0.01 vs CTR NCD, #P<0.05 vs CTR HFD. Triglycerides (TG) (c), non-esterified fatty acid (NEFA) (d) and cholesterol (TC) (e) in liver of mice (n=10). **P<0.01, ***P<0.001 vs CTR NC,

#P<0.05, ##P<0.01 vs CTR HFD. (f) Hematoxylin and eosin (H&E, top)-stained and Oil Red O (bottom)-stained liver sections from mice. Scale bar, 20 μm. Quantitative analysis (right) of the mean Oil-red O-staining area (n =10). **P<0.01 vs CTR HFD. (g) Relative mRNA levels of indicated molecules in the liver of mice (n=5). *P<0.05, **P<0.01, ***P<0.001, ****P<0.0001 vs CTR HFD. (h) Serum levels of alanine transaminase (ALT) and aspartate aminotransferase (AST) (n=10). *P<0.05, **P<0.01 vs CTR NCD, #P<0.05 vs CTR HFD.

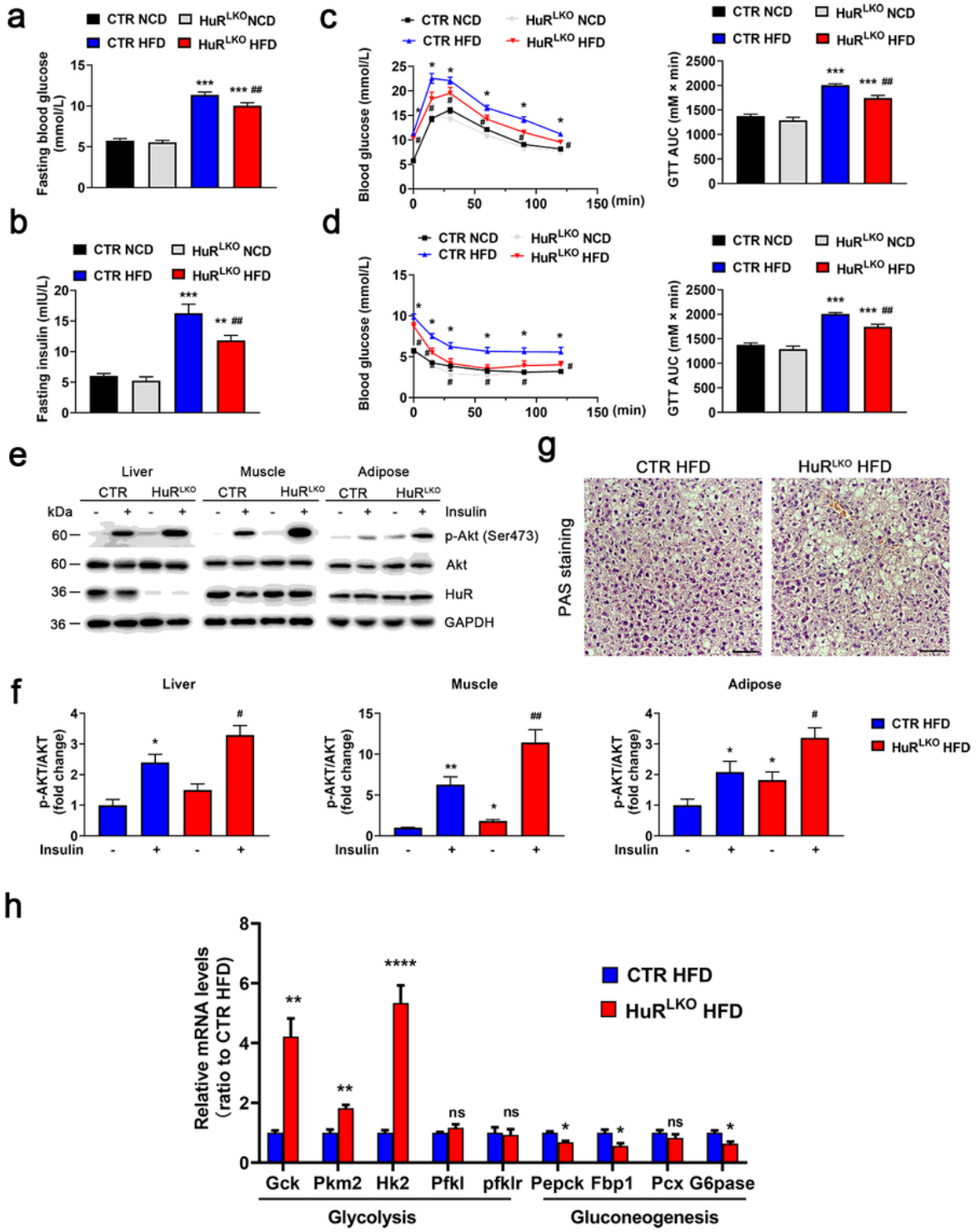

Figure 4

Hepatic specific HuR deletion alleviated HFD-impaired glucose tolerance. Fasting glucose levels (a) and fasting insulin levels (b) of HuRLKO and CTR mice in response to HFD (n = 10). **P<0.01, ***P<0.001 vs CTR NCD, ##P<0.01 vs CTR HFD. Glucose tolerance test (GTT) (c) and insulin tolerance test (ITT) (d) in HuRLKO and CTR mice after NCD or HFD feeding for 24 weeks. The corresponding areas under the curve (AUC) of blood glucose levels (right). (n=8). *P<0.05 ***P<0.001 vs CTR NCD, #P<0.05 ##P<0.01 vs CTR HFD. (e-f) Western blot analysis of Akt phosphorylation in tissues of control and HuRLKO mice with HFD (n=5). *P<0.05, **P<0.01 vs CTR HFD saline, #P<0.05, ##P<0.01 vs CTR HFD+insulin. (g) Periodic acid-Schiff (PAS)-stained liver sections from HuRLKO and CTR mice after HFD feeding for 24 weeks. Scale bar, 20 μm. (h) Relative mRNA levels of genes involved in hepatic glycolysis and gluconeogenesis in HuRLKO and CTR mice with HFD feeding (n=5). *P<0.05, **P<0.01, ****P<0.0001 vs CTR HFD.

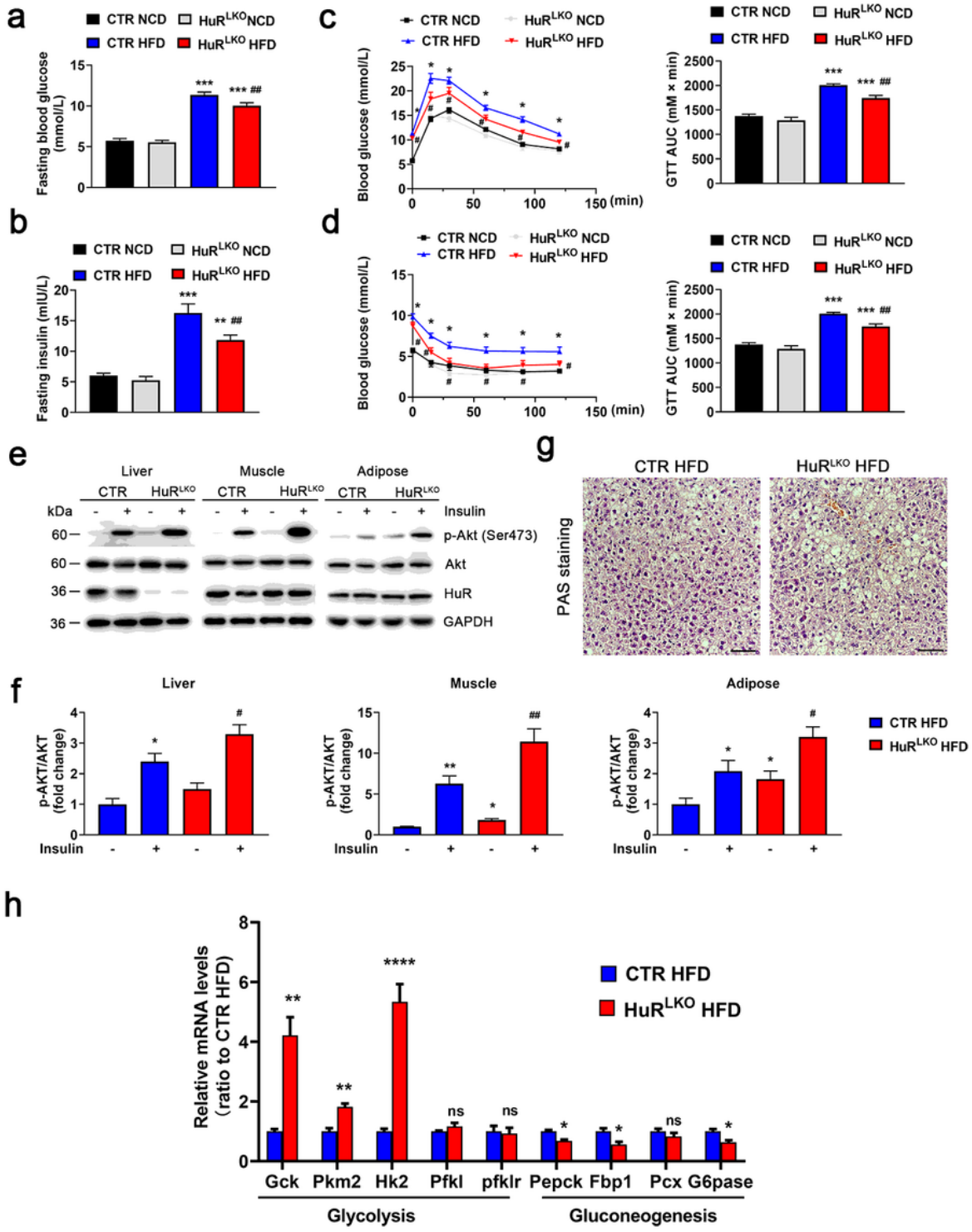

Figure 4

Hepatic specific HuR deletion alleviated HFD-impaired glucose tolerance. Fasting glucose levels (a) and fasting insulin levels (b) of HuRLKO and CTR mice in response to HFD (n = 10). **P<0.01, ***P<0.001 vs CTR NCD, ##P<0.01 vs CTR HFD. Glucose tolerance test (GTT) (c) and insulin tolerance test (ITT) (d) in HuRLKO and CTR mice after NCD or HFD feeding for 24 weeks. The corresponding areas under the curve (AUC) of blood glucose levels (right). (n=8). *P<0.05 ***P<0.001 vs CTR NCD, #P<0.05 ##P<0.01 vs CTR

HFD. (e-f) Western blot analysis of Akt phosphorylation in tissues of control and HuRLKO mice with HFD (n=5). *P<0.05, **P<0.01 vs CTR HFD saline, #P<0.05, ##P<0.01 vs CTR HFD+insulin. (g) Periodic acid-Schiff (PAS)-stained liver sections from HuRLKO and CTR mice after HFD feeding for 24 weeks. Scale bar, 20 μm. (h) Relative mRNA levels of genes involved in hepatic glycolysis and gluconeogenesis in HuRLKO and CTR mice with HFD feeding (n=5). *P<0.05, **P<0.01, ****P<0.0001 vs CTR HFD.

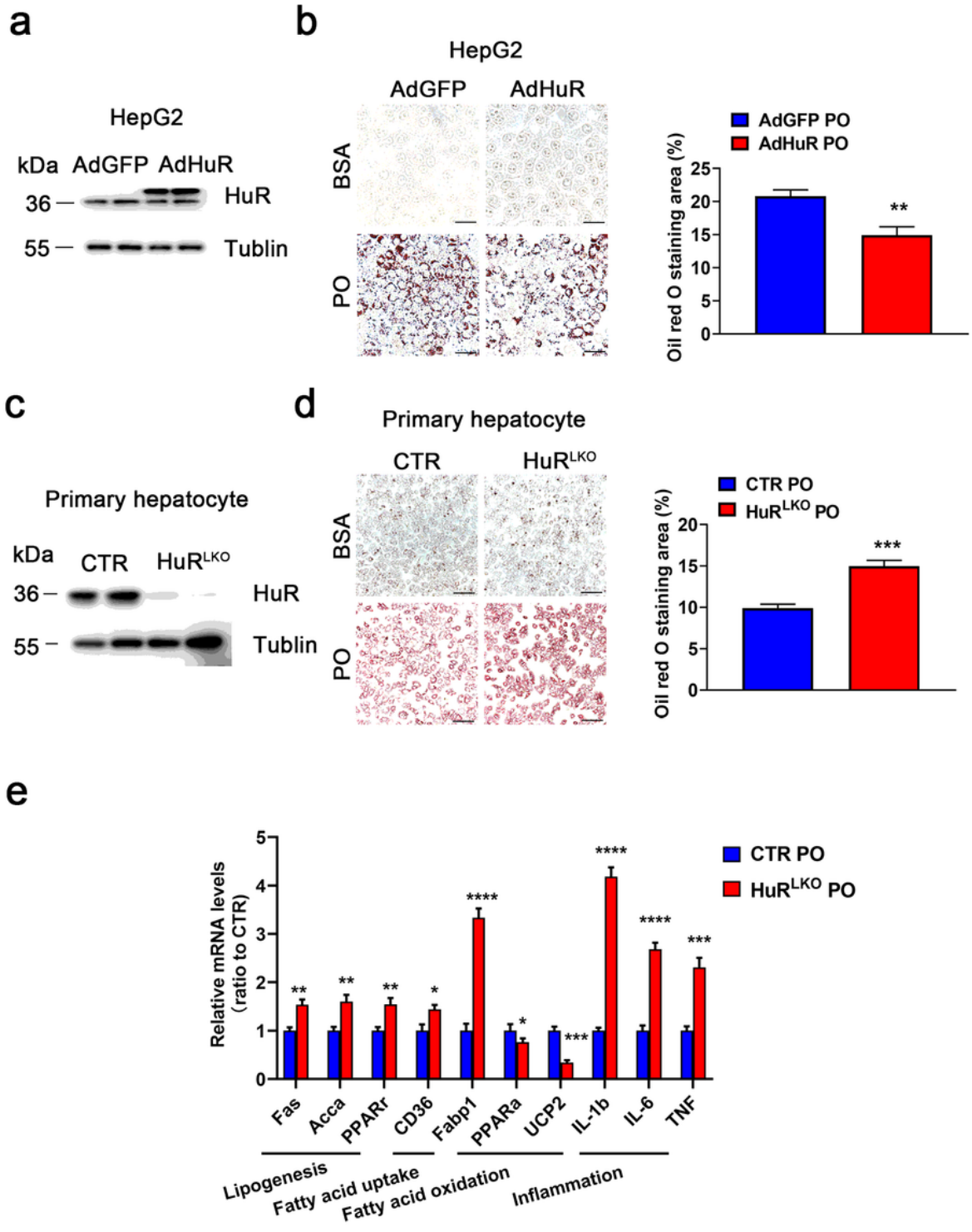

Figure 5

HuR inhibited lipid accumulation in hepatocytes. (a) Western blot analysis of HuR protein expression of HepG2 cells infected with adenovirus expressing GFP or HuR for 24 h. (b) After infection with adenovirus for 24 h, HepG2 cells were treated with BSA or PO for 24 h, followed by Oil-red O staining (n=5). Scale bar, 50 μm. **P<0.01 vs AdGFP PO. (c) Western blot analysis of HuR protein level in primary hepatocytes from HuRLKO and CTR mice. (d) Primary hepatocytes were treated with BSA or PO for 24 h, followed by Oil-red O staining (n=5). Scale bar, 100 μm. ***P<0.001 vs CTR PO. (e) Relative mRNA expression of the indicated molecules in primary hepatocytes treated with PO (n=5). *P<0.05, **P<0.01, ***P<0.001, ****P<0.0001 vs CTR PO.

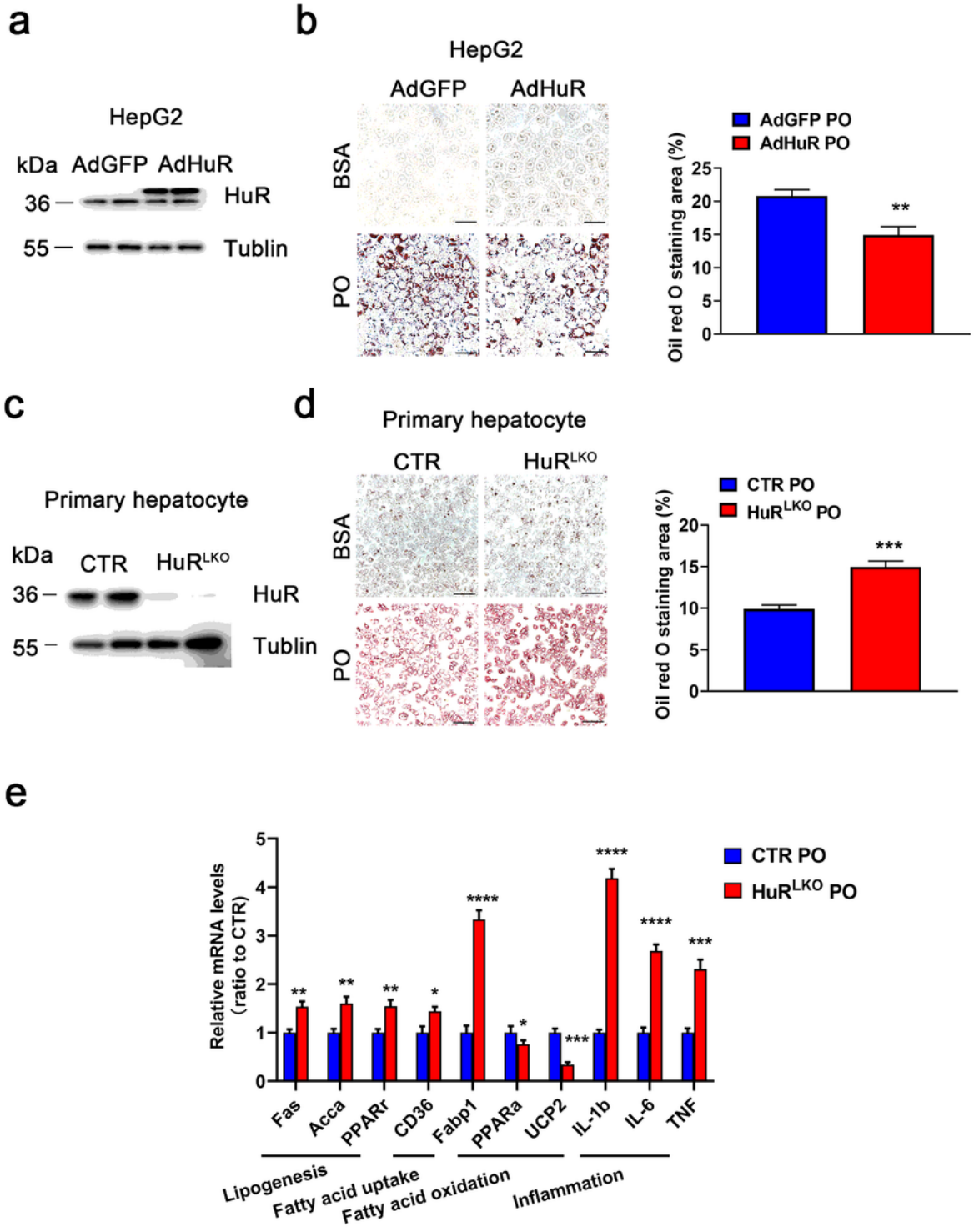

Figure 5

HuR inhibited lipid accumulation in hepatocytes. (a) Western blot analysis of HuR protein expression of HepG2 cells infected with adenovirus expressing GFP or HuR for 24 h. (b) After infection with adenovirus for 24 h, HepG2 cells were treated with BSA or PO for 24 h, followed by Oil-red O staining (n=5). Scale bar, 50 μm. **P<0.01 vs AdGFP PO. (c) Western blot analysis of HuR protein level in primary hepatocytes from HuRLKO and CTR mice. (d) Primary hepatocytes were treated with BSA or PO for 24 h, followed by Oil-red

O staining (n=5). Scale bar, 100 μm. ***P<0.001 vs CTR PO. (e) Relative mRNA expression of the indicated molecules in primary hepatocytes treated with PO (n=5). *P<0.05, **P<0.01, ***P<0.001, ****P<0.0001 vs CTR PO.

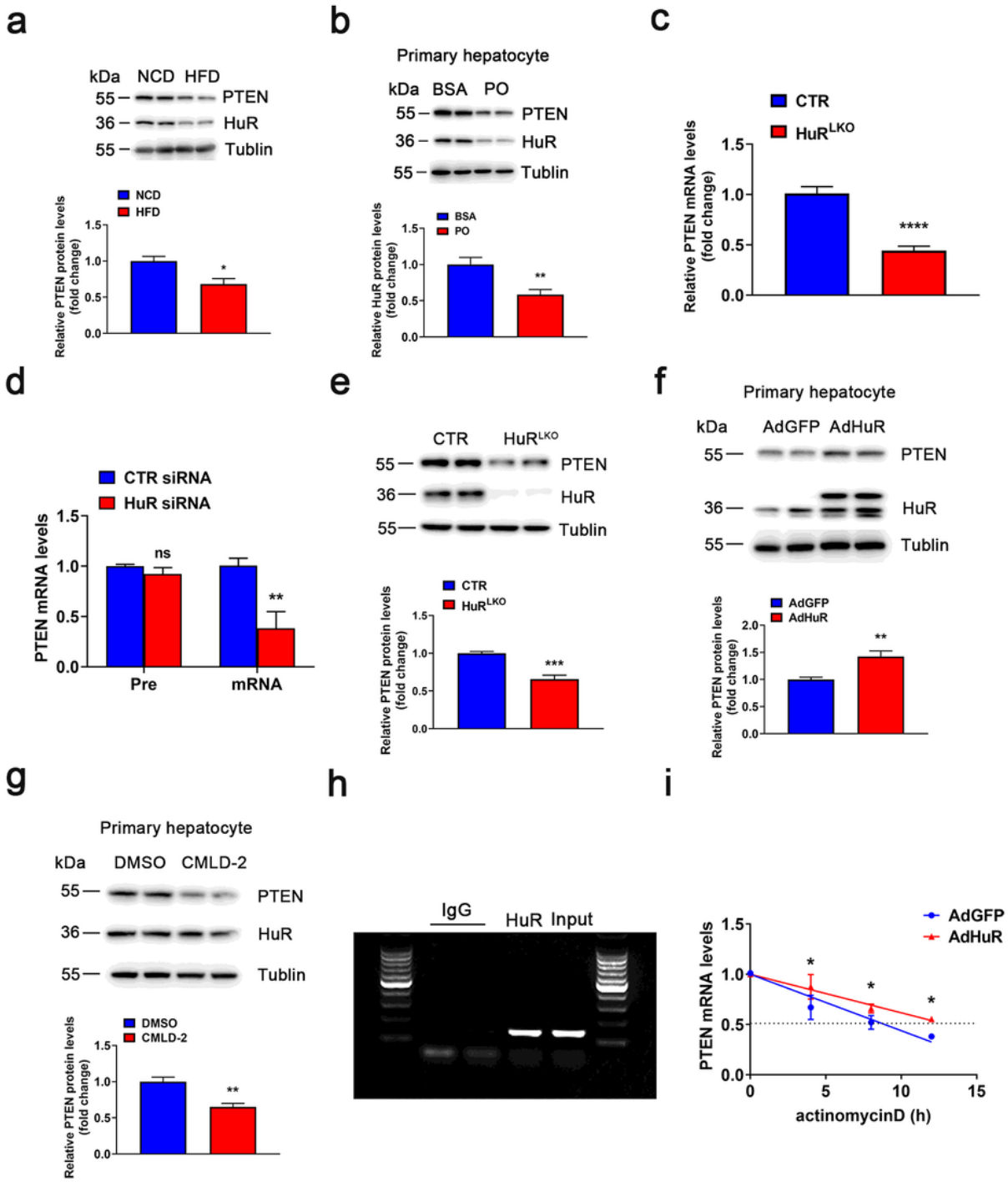

Figure 6

HuR regulates PTEN mRNA stability. (a) Western blot analysis of PTEN protein level in liver of NCD- or HFD-fed CTR and HuRLKO mice (n=5). *P<0.05 vs NCD. (b) Western blot analysis of PTEN protein level in

primary hepatocytes stimulated with BSA or PO for 24 h (n=5). **P<0.01 PO vs BSA. (c) qPCR analysis to detect PTEN mRNA level in liver of CTR and HuRLKO mice (n=5). **** P<0.0001 vs CTR. (d) qPCR analysis to detect PTEN pre-mRNA and mature mRNA levels in primary hepatocytes transfected with CTR siRNA or HuR siRNA (n=3). **P<0.01 vs. CTR siRNA. (e) Western blot analysis of PTEN protein level in liver of CTR and HuRLKO mice (n=5). ***P<0.001 vs CTR. (f) Western blot analysis of PTEN protein level in primary hepatocytes infected with adenovirus expressing GFP or HuR for 24 h (n=5). **P<0.01 vs AdGFP. (g) Primary hepatocytes were stimulated with DMSO or CMLD-2 (30 μM) for 24h. Western blot analysis of PTEN protein level and quantification (n= 4). **P<0.01 vs DMSO. (h) RNA immunoprecipitation with anti-HuR antibody or control IgG. (i) Primary hepatocytes infected with adenovirus expressing GFP or HuR for 24 h were stimulated with 10 μg/mL actinomycin D for the indicated time. Quantitative PCR analysis of PTEN mRNA level (n=3). *P<0.05 vs AdGFP.

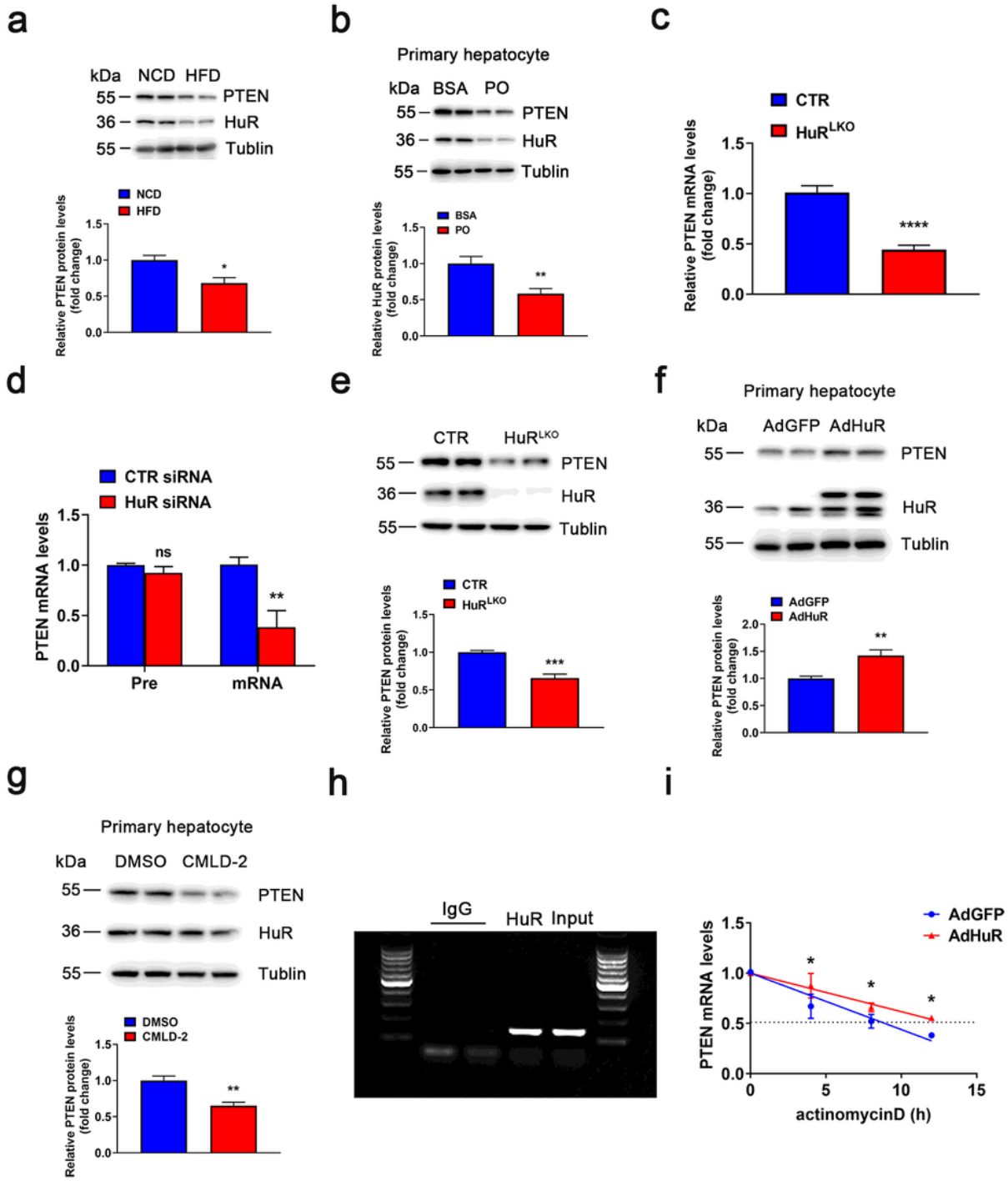

Figure 6

HuR regulates PTEN mRNA stability. (a) Western blot analysis of PTEN protein level in liver of NCD- or HFD-fed CTR and HuRLKO mice (n=5). *P<0.05 vs NCD. (b) Western blot analysis of PTEN protein level in primary hepatocytes stimulated with BSA or PO for 24 h (n=5). **P<0.01 PO vs BSA. (c) qPCR analysis to detect PTEN mRNA level in liver of CTR and HuRLKO mice (n=5). **** P<0.0001 vs CTR. (d) qPCR analysis to detect PTEN pre-mRNA and mature mRNA levels in primary hepatocytes transfected with CTR

siRNA or HuR siRNA (n=3). **P<0.01 vs. CTR siRNA. (e) Western blot analysis of PTEN protein level in liver of CTR and HuRLKO mice (n=5). ***P<0.001 vs CTR. (f) Western blot analysis of PTEN protein level in primary hepatocytes infected with adenovirus expressing GFP or HuR for 24 h (n=5). **P<0.01 vs AdGFP. (g) Primary hepatocytes were stimulated with DMSO or CMLD-2 (30 μM) for 24h. Western blot analysis of PTEN protein level and quantification (n= 4). **P<0.01 vs DMSO. (h) RNA immunoprecipitation with anti-HuR antibody or control IgG. (i) Primary hepatocytes infected with adenovirus expressing GFP or HuR for 24 h were stimulated with 10 μg/mL actinomycin D for the indicated time. Quantitative PCR analysis of PTEN mRNA level (n=3). *P<0.05 vs AdGFP.

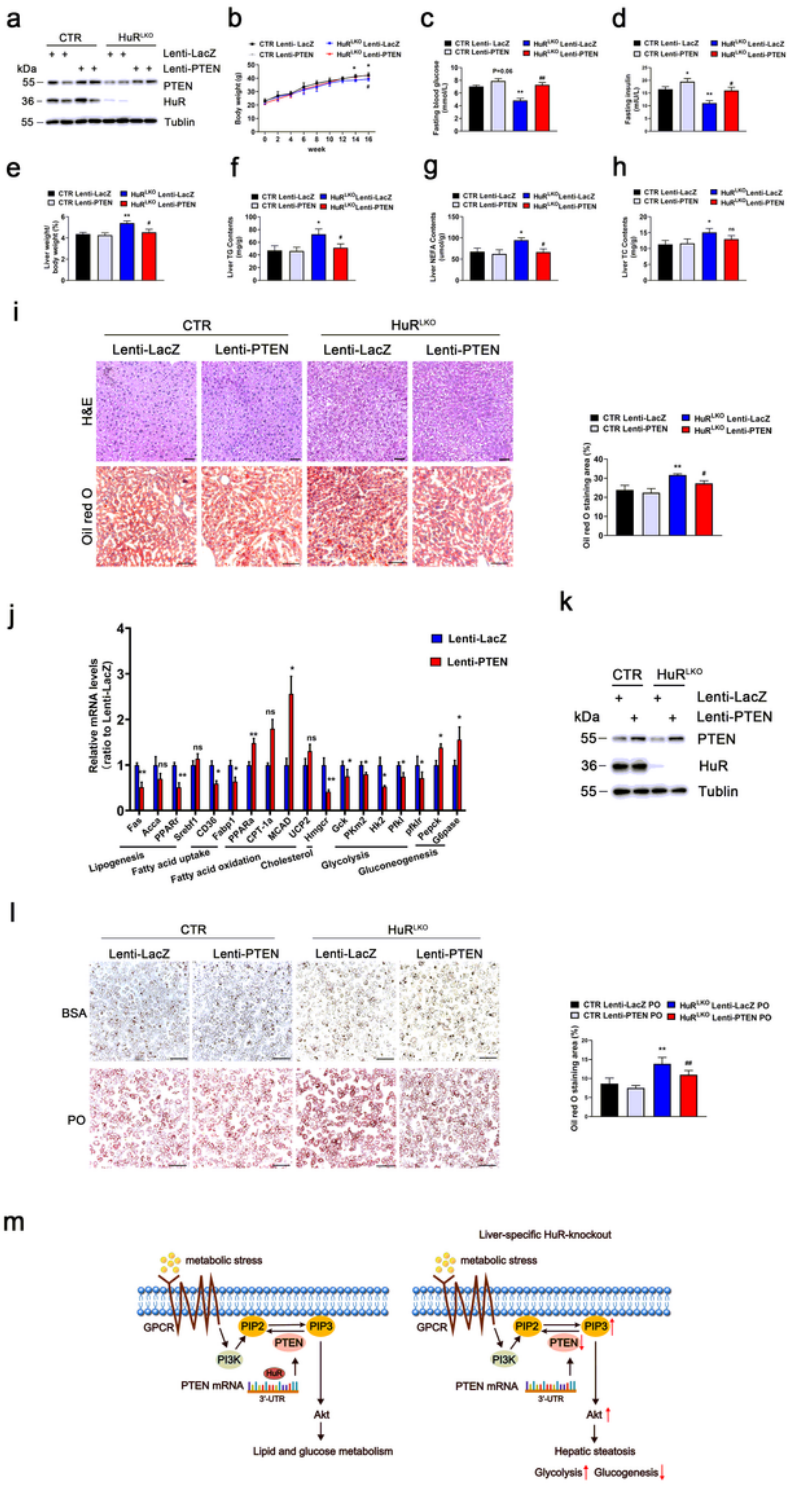

Figure 7

HuR regulates hepatocyte steatosis through PTEN. (a) HuRLKO and CTR mice were injected with LacZ or PTEN lentivirus (1.0E+07TU per mice) and challenged with an HFD. Western blot analysis of PTEN protein level. (b) Body weight of mice in different groups (n=5). *P<0.05 vs CTR Lenti-LacZ, #P<0.05 vs HuRLKO Lenti-LacZ. (c) Fasting glucose levels in liver of mice (n=5). **P<0.01 vs CTR Lenti-LacZ, ##P<0.01 vs HuRLKO Lenti-LacZ. (d) Fasting insulin levels in liver of mice (n=5). *P<0.05, **P<0.01 vs CTR Lenti-LacZ,

#P<0.05 vs HuRLKO Lenti-LacZ. (e) Liver weight to body weight ratio of mice (n=5). **P<0.01 vs CTR Lenti-LacZ, #P<0.05 vs HuRLKO Lenti-LacZ. TG (f), NEFA (g), and TC (h) levels in liver of mice (n=5). *P<0.05 vs CTR Lenti-LacZ, #P<0.05 vs HuRLKO Lenti-LacZ. (i) H&E (top)-stained and Oil-red O (bottom)-stained liver sections from mice. Scale bar, 50 μm. Quantitative analysis (right) of mean Oil-red O staining area (n =5). **P<0.01 vs CTR Lenti-LacZ, #P<0.05 vs HuRLKO Lenti-LacZ. (j) Relative mRNA levels of the indicated molecules in livers of mice (n=5). *P<0.05, **P<0.01 vs HuRLKO Lenti-LacZ. (k) Western blot analysis of PTEN protein level. (l) CTR and HuRLKO primary hepatocytes infected with PTEN lentivirus were treated with BSA or PO for 24 h, followed by Oil-red O staining (n=3). Scale bar, 100 μm. **P<0.01 vs CTR Lenti-LacZ PO, ##P<0.01 vs HuRLKO Lenti-LacZ PO. (m) Schematic diagram about the mechanism of HuR in lipid and glucose metabolism.

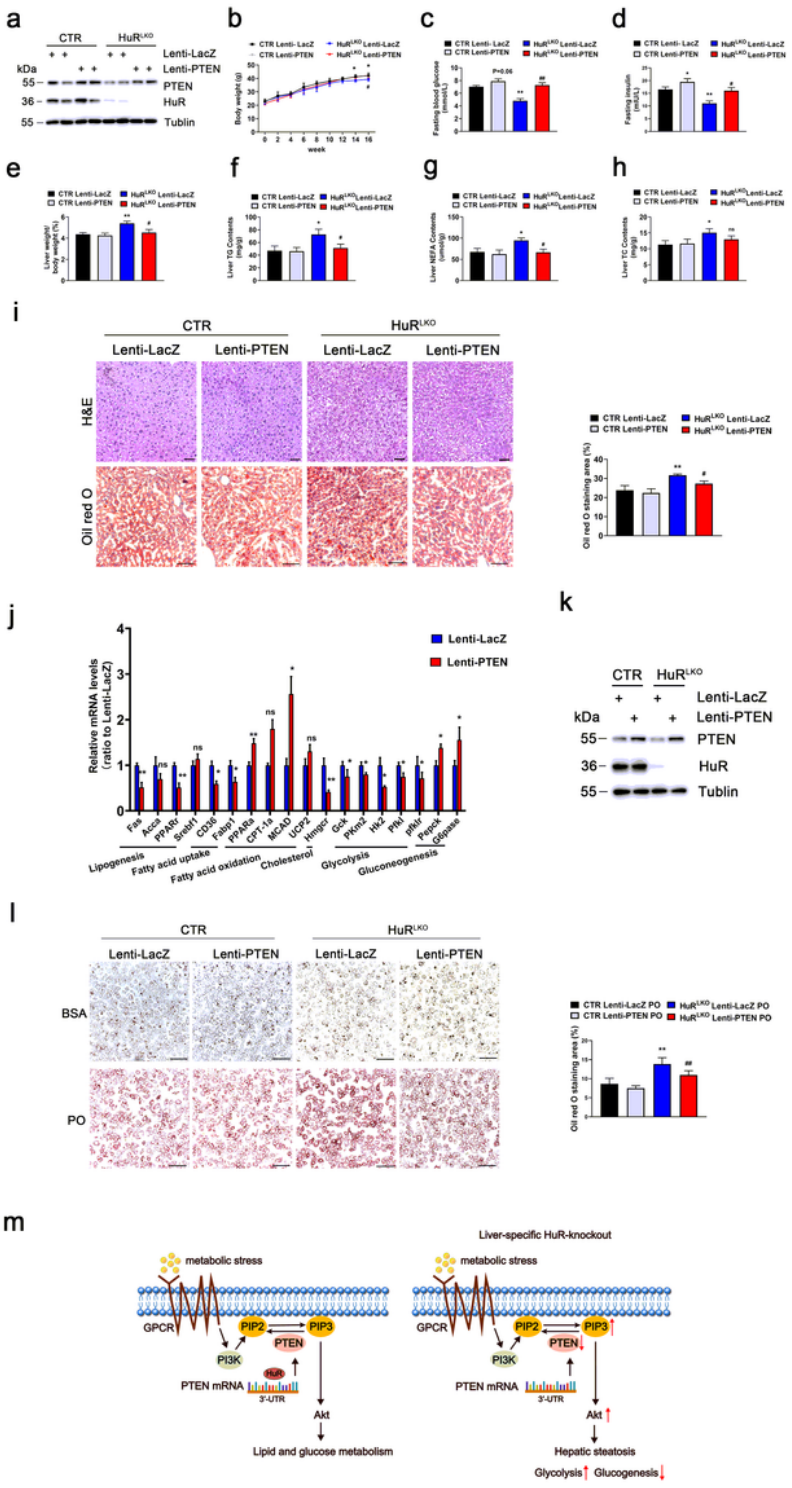

Figure 7

HuR regulates hepatocyte steatosis through PTEN. (a) HuRLKO and CTR mice were injected with LacZ or PTEN lentivirus (1.0E+07TU per mice) and challenged with an HFD. Western blot analysis of PTEN protein level. (b) Body weight of mice in different groups (n=5). *P<0.05 vs CTR Lenti-LacZ, #P<0.05 vs HuRLKO Lenti-LacZ. (c) Fasting glucose levels in liver of mice (n=5). **P<0.01 vs CTR Lenti-LacZ, ##P<0.01 vs HuRLKO Lenti-LacZ. (d) Fasting insulin levels in liver of mice (n=5). *P<0.05, **P<0.01 vs CTR Lenti-LacZ,

#P<0.05 vs HuRLKO Lenti-LacZ. (e) Liver weight to body weight ratio of mice (n=5). **P<0.01 vs CTR Lenti-LacZ, #P<0.05 vs HuRLKO Lenti-LacZ. TG (f), NEFA (g), and TC (h) levels in liver of mice (n=5). *P<0.05 vs CTR Lenti-LacZ, #P<0.05 vs HuRLKO Lenti-LacZ. (i) H&E (top)-stained and Oil-red O (bottom)-stained liver sections from mice. Scale bar, 50 μm. Quantitative analysis (right) of mean Oil-red O staining area (n =5). **P<0.01 vs CTR Lenti-LacZ, #P<0.05 vs HuRLKO Lenti-LacZ. (j) Relative mRNA levels of the indicated molecules in livers of mice (n=5). *P<0.05, **P<0.01 vs HuRLKO Lenti-LacZ. (k) Western blot analysis of PTEN protein level. (l) CTR and HuRLKO primary hepatocytes infected with PTEN lentivirus were treated with BSA or PO for 24 h, followed by Oil-red O staining (n=3). Scale bar, 100 μm. **P<0.01 vs CTR Lenti-LacZ PO, ##P<0.01 vs HuRLKO Lenti-LacZ PO. (m) Schematic diagram about the mechanism of HuR in lipid and glucose metabolism.

Supplementary Files

This is a list of supplementary files associated with this preprint. Click to download.

- Graphicalabstract.jpeg
- Graphicalabstract.jpeg
- SupplementaryInformation.docx
- SupplementaryInformation.docx